

Numerical Prediction of Ship Resistance in Calm Water by Using RANS Method

T.N. Tu, N.T.H. Phuong, V. Tuan Anh, V.M. Ngoc, P.T.T. Hai and C.H. Chinh
Faculty of Shipbuilding, Vietnam Maritime University, Lach Tray Street 484, Hai Phong, Vietnam

Abstract: It is essential to predict the ship resistance during the process of design and optimization of the ship hull form with respect to the resistance reduction. With the development of computational resources, Computational Fluid Dynamics (CFD) has been being widely used in calculating the ship resistance. However, level of accuracy of the numerical simulation significantly depends on human skills. This study is aimed to predict ship resistance, sinkage and trim in calm water by using unsteady RANS method. The effects of grids on simulation results is analyzed by performing some simulations on a sequence of systematically refined grid. The study comprises the numerical results of calm water calculation for the DTMB Model with available experimental results. The simulation is performed by using commercial solver Star-CCM+.

Key words: Ship resistance, CFD, RANS, grid convergence, calm water

INTRODUCTION

In order to achieve the reliable result generally for ship hydrodynamic derivatives and particularly for ship resistance, the designers need to execute the model tests in towing tank. The obtained results then will be transformed to the full scale of the designed ship. Because model testing is costly and time-consuming, so, this method is only used after the stage of alternative design, at which dimensions as well as lines plan of ship have been already optimally chosen.

Now a days with the development of computational resources, calculating the ship resistance using Computational Fluid Dynamics (CFD) in preliminary design to optimise the hull shape of ship has been being widely used because of relatively accurate result in comparison with model testing. Some useful results using RANS method with different turbulence models for calculating ship resistance have been achieved. Shia *et al.* (2012) used RANS with SST (Shear Stress Transport) $k-\omega$ turbulence model to evaluate the ship resistance for DTMB INSEAN 2340 Model hull. The ship were simulated at seven Froude numbers from 0.15-0.45 using 1.15 million cells in simulation. The error between predicted resistance and experimental data ranges from 1.15-3.56. Wu *et al.* (2000) used RANS with $k-\epsilon$ two-equation turbulence model to predict the ship resistance for model DTMB 5415 surface ship. The ship were simulated at three Froude numbers: 0.138, 0.28, 0.41 using 660.500 cells in simulation. The error between predicted resistance and experimental data range from 0.12-2.36. Ahmed (2011) used RANS with standard $k-\epsilon$ turbulence model to compute ship resistance for model

DTMB 5415. The ship were simulated at two Froude numbers. The numerical results obtained are quite precise compared to the experimental data. Sang-Hull Park (Qiu, 2014) used commercial CFD code of the STAR-CCM+ to evaluate the ship resistance for KCS by using RANS with Reynold stress model. The predicted total resistance coefficient show good agreement with experimental result. Saha and Miazee (2017) determined different hydrodynamic values such as resistance, sinkage and trim for a container ship using CFD Software SHIPFLOW based on RANS method. This ship was simulated in deep water at different Froude numbers including service speed. The viscous, wave and total resistance were calculated for speeds ranging from 8.0-10.0 knots. The computed values were illustrated being in good agreement with the experimental values. Islam *et al.* (2017) calculated resistance for KCS Model in calm water at six Froude numbers using a CFD solver named Ship Motion which is based on the Reynolds Average Navier-Stokes method (RANS). The average deviation of total drag is found to be around 2% which is very reasonable considering the used mesh resolution of around 1 million.

The published literatures above played an important role for the further researches using RANS method with different turbulence models to simulate ship resistance. However, they have not analysed systematically the influence of mesh such as mesh density as well as grid arrangement on the achieved results which plays an important role in the stage of alternative design due to the fact that in this stage we do not have the model test results to compare with computed values. Therefore, it is necessary to take into account these mentioned issues in

order to avoid the errors caused by mesh generation when given physical models. This is also the content that will be presented in this study.

MATERIALS AND METHODS

Mathematical model: To investigate the ship resistance, the flow around the ship is modeled using the incompressible, RANS equations:

$$\frac{\partial u_i}{\partial x_i} = 0 \tag{1}$$

$$\frac{\partial u_i}{\partial t} + \frac{\partial}{\partial x_j} (u_i u_j) = -\frac{1}{\rho} \frac{\partial P}{\partial x_i} + \frac{\partial}{\partial x_j} \left(\nu \frac{\partial u_i}{\partial x_j} - u_i' u_j' \right) + f_i \tag{2}$$

Where:

- u_i = The temporal averaged velocity component
- P = The Pressure
- f_i = The body force component of fluid
- ρ = The fluid density
- ν = The kinematic viscosity
- u_i' = The fluctuation velocity component
- $-u_i' u_j'$ = The Reynolds stress

The VOF method is used to simulate the free surface, transport equations of volume fraction C_q can also be solved by governing equations:

$$\frac{\partial C_q}{\partial t} + u_i \frac{\partial C_q}{\partial x_i} = 0 \tag{3}$$

The standard k-ε turbulence model is used instead to minimize unknowns and presenting a set of equation which can be applied to large number of turbulence applications. Turbulent kinetic energy k and turbulent dissipation ε are given by following equation:

$$\frac{\partial(\rho k)}{\partial t} + \frac{\partial(\rho k u_i)}{\partial x_i} = \frac{\partial}{\partial x_j} \left[\frac{\mu_t}{\sigma_k} \frac{\partial k}{\partial x_j} \right] + 2\mu_t E_{ij} E_{ij} - \rho \epsilon \tag{4}$$

$$\frac{\partial(\rho \epsilon)}{\partial t} + \frac{\partial(\rho \epsilon u_i)}{\partial x_i} = \frac{\partial}{\partial x_j} \left[\frac{\mu_t}{\sigma_\epsilon} \frac{\partial \epsilon}{\partial x_j} \right] + C_{1\epsilon} \frac{\epsilon}{k} 2\mu_t E_{ij} E_{ij} - C_{2\epsilon} \rho \frac{\epsilon^2}{k} \tag{5}$$

Where:

- u_i - Velocity component in corresponding direction
- E_{ij} - Component of rate of deformation
- μ_t - Eddy viscosity

$$\mu_t = \rho C_\mu \frac{k^2}{\epsilon} \tag{6}$$

The equations also consist of some adjustable constants σ_k , σ_ϵ , C_μ and $C_{1\epsilon}$. The values of these constants have been arrived at by numerous iterations of data fitting for a wide range of turbulent flows. These are as follows: $C_\mu = 0.09$; $\sigma_k = 1.0$; $\sigma_\epsilon = 1.3$; $C_{1\epsilon} = 1.44$

The turbulence model chosen for use in this study was a standard k-ε model due to it has been extensively used for industrial applications according to ITTC 2014 (Anonymous, 2017). Additionally, Querard *et al.* (2008) claims that the k-ε model is quite economical in terms of CPU time, compared to, for example, the SST turbulence model which increases the required CPU time by nearly 25%. The majority of the numerical methods presented in the 2010 Gothenburg workshop used the k-ε turbulence model. At the workshop, most of the studies performed using Star-CCM+ as a RANS solver employ the standard k-ε model as is used in this study.

Numerical simulations

Reference vessel: The vessel under study in this study is a US Navy Combatant DTMB shown in Fig. 1. The main reason for using this hull is that extensive model test data exists for resistance at different Froude numbers (Olivieri *et al.*, 2001). The computation were carried out at model scale $\lambda = 24.824$.

Test case: Computations were performed at design draft ($T = 0.248$) with five value of Froude numbers: 0.20, 0.25, 0.3, 0.35, 0.40.

Computation method: The commercial package Star-CCM+ from CD-Adapco was used for computation. For ship resistance calculation, only the port side of the hull is simulated due to model's symmetry condition.

Solution domain and boundary conditions: Based on the recommendations and applications reported in CD-ADAPCO, the external boundaries of the domain was located as the follows: inlet boundary is located at 1.5 Lpp from FP while outlet is located at 2.5 Lpp after AP.



Fig. 1: Geometry of US Navy combatant DTMB

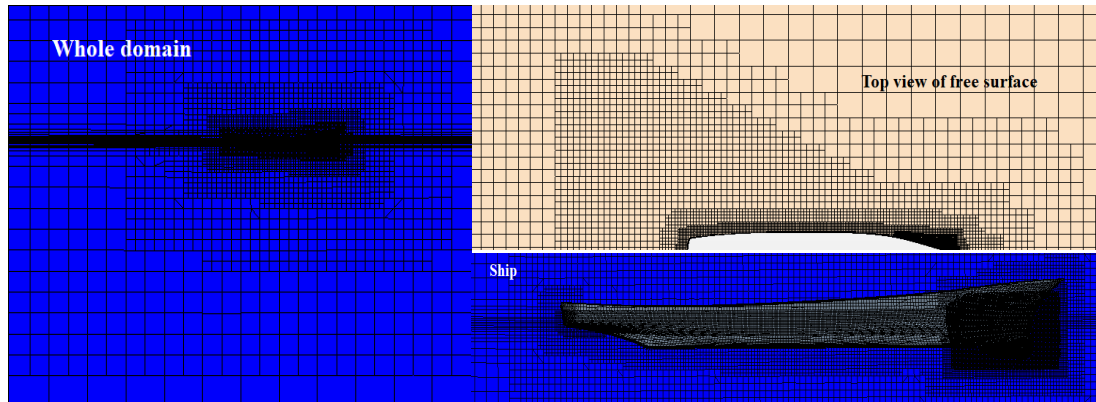


Fig. 2: The structure of coarse mesh for whole domain, around the ship and near free surface in the wake and in the wave zone

Table 1: Main particulars of the DTMB

Description	Ship	Model
Scale factor (λ)	-	24.824
Length between perpendiculars (L_{pp} (m))	142.0	5.720
Length at Water Level (L_{WL} (m))	142.0	5.720
Breadth (B (m))	18.9	0.760
Draft (T (m))	6.16	0.248
Volume (Δ (m ³))	8425.4	0.549
Wetted Surface (SW (m ²))	2949.5	4.786
Longitudinal Center of Buoyancy (LCB (% L_{pp}), fwd+)	-0.683	0.506

Bottom and top boundaries are located at 2.5 and 1.25 L_{pp} away from the free surface, respectively. Lateral boundary is located at 2.5 L_{pp} away from the midship plane (Table 1).

Boundary condition: Inlet condition were used on inlet, top and bottom. No slip condition on the hull. At outflow the hydrostatic pressure was specified. Slip condition was used on the side walls. The free surface lies at $z = 0$. The ship stern (aft perpendicular) is located at $x = 0$ and the bow is $x = L_{pp}$.

Physics modeling: To model fluid flow, the solver employed uses a finite volume method which uses the integral form of the conservation equations and divides the computational domain into a finite number of adjoining control volumes.

The 6-DOF motion and VOF multiphase model were employed handle heave and pitch motions and also the free surface wave flow around hull. Motion of the hull was captured during the computation by using Dynamic Fluid Body Interaction (DFBI) with 2DOF (Y-axis rotation and Z-direction motion was allowed for the hull). Wave damping in the region distanced about 1.25 L was applied to reduce the resistance force fluctuation due to boundary condition.

Mesh generation: In this study, trimmed hexahedral grids and prism layers along wall were used. The grid near the free surface was refined to capture elevation of the waves precisely. The grid generation process is driven by specifying base mesh size, relative to which all spacing are defined. Finer meshes of the same topology are then automatically created by just reducing the base size. In order to avoid using fine grid where it is not necessary (in from and behind the ship and larger distance below, above on each side the hull), local volume were created to sonar dome and assigned particular cell size, resulting in mesh structure shown in Fig. 2 for the coarsest mesh.

RESULTS AND DISCUSSION

Grid convergence study: The first step of research is to determine mesh density for convergence studying at which the difference of total resistance coefficient C_T reaches sufficiently low value while maintaining plausible computational effort. Grid studies have been conducted using three grids with non-integer grid refinement ratio $r_g = \sqrt{2}$ (the value has been recommended by ITTC-Quality Manual 7.5-03-01-01, 2008) such as coarse (grid#3), medium (grid#2) and fine grid (grid#1) system corresponding to the cells are 596480, 1308879 and 3245565, respectively. Mesh refinement is done by reducing the cell size in all directions outside prism layer. The idea here was to keep the same y^+ values at near-wall cells about 40 over the largest part of the wetted hull surface for the all three case. The mesh convergence test was carried out at $Fr = 0.25$.

The validation is performed on the comparison error between experimental values D (EFD) and CFD simulation values, S in this study, defined as:

Table 2: Ship resistance at Fr = 0.25 with different grids

Parameters	EFD (D)	V&V study			$\epsilon_{32\%}$	$\epsilon_{12\%}$	R
		Grid#3	Grid#2	Grid#1			
$C_T \times 10^3$							
Value	4.070	4.264	4.163	4.140	-1.03	-0.50	0.485
E%D	/	-4.320	-2.280	-1.720			
$C_F \times 10^3$							
Value	/	3.032	3.018	3.008	-0.45	-0.34	0.756
E%D	/	/	/	/			
$C_P \times 10^3$							
Value	/	1.174	1.145	1.134	-2.58	-0.94	0.364
E%D	/	/	/	/			

Table 3: Ship resistance, trim and sinkage results in comparison to experimental values

Parameters	Fr = 0.2	Fr = 0.25	Fr = 0.3	Fr = 0.35	Fr = 0.4
$C_T \times 10^3$					
EFD(D)	3.95000	4.07000	4.43000	4.84000	6.32000
CFD(S)	4.01000	4.14000	4.28000	4.92000	6.14000
Relative error (%)	-1.52000	-1.72000	-1.18000	-1.65000	2.85000
Sinkage/Lpp					
EFD(D)	-0.00100	-0.00140	-0.00210	-0.00315	-0.00449
CFD(S)	-0.00107	-0.00152	-0.00219	-0.00336	-0.00430
Relative error (%)	-7.00000	-8.75000	-4.17000	-6.67000	-4.28000
Trim (°)					
EFD(D)	0.06100	0.0850	0.10800	0.06900	-0.24200
CFD(S)	0.06400	0.0918	0.11620	0.07200	-0.24800
Relative error (%)	-4.92000	-8.0000	-7.59000	-4.34000	-2.47000

$$E\%D = \frac{(D-S)}{D} \cdot 100\%$$

The solution changes between two simulations such as fine-medium ϵ_{12} and medium coarse ϵ_{23} , the convergence factor R are defined as follow:

$$\epsilon_{12} = S_1 - S_2; \epsilon_{23} = S_2 - S_3$$

Table 2 presents the results for resistance coefficients resulting from three grids resolutions at Fr = 0.25. The comparison shows quite good agreement, especially, for the fine mesh simulative results (the error only 1.72%). For all six variables, the convergence factors are between 0 and 1 which imply that the simulation is monotonically converged. The solution change between the grids 1 and 2 (ϵ_{12}) is two time smaller than between the grids 2 and 3 (ϵ_{23}) and is smaller -0.94% for all resistance coefficients, so that, further grid refinement would be desirable. Therefore, the fine mesh was chosen for the further analysis.

Numerical simulation results: Table 3 and Fig. 3-5 shows the comparison of predicted and measured total ship resistance coefficient, trim and sinkage with Froude number range (ranging) from 0.2-0.4. The predicted total ship resistance coefficient agrees well with the experiment data with tolerance is <3% for the total ship resistance coefficient.

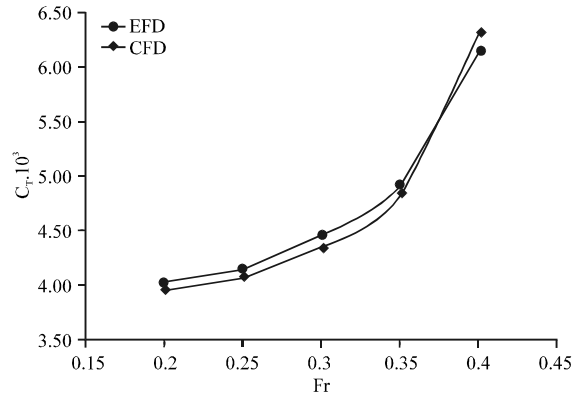


Fig. 3: Comparison of predicted and measured total resistance coefficient

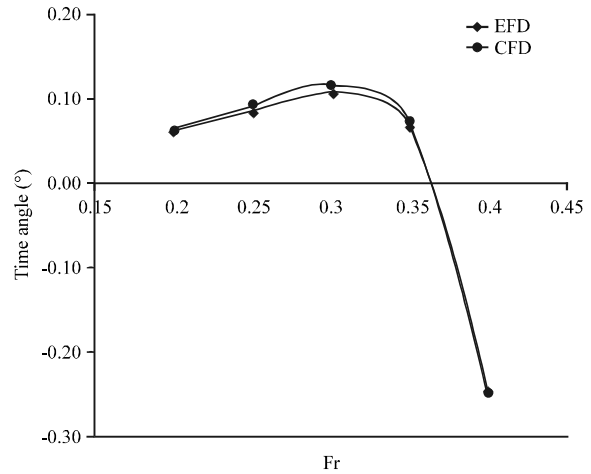


Fig. 4: Comparison of predicted and measured trim

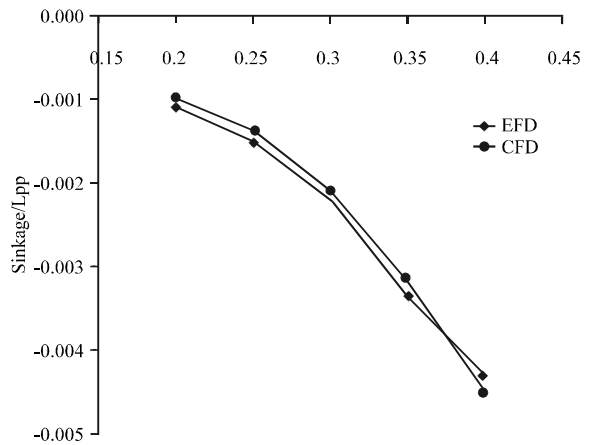


Fig. 5: Comparison of predicted and measured sinkage

The trim and sinkage and trim differ more from experimental data. The errors in trim angle are -4.92, -8.00,

-7.59, -4.34 and -2.47 (from the lowest to the highest Froude number). The discrepancies in sinkage are -7.00%, -8.75, -4.17, -6.67, -4.28 in order of increasing Froude numbers.

CONCLUSION

A method for unsteady RANS simulation for predicting ship resistance is proposed. A successively refined grid study has been attempted. Good convergence trend has been obtained for the resistance prediction considering the dynamic sinkage and trim. The predictions of the ship resistance, trim and sinkage of the DTMB Model enjoy high level of accuracy.

ACKNOWLEDGEMENT

The researchers are grateful to the Vietnam Maritime University for providing necessary research facilities during current research work.

REFERENCES

- Ahmed, Y.M., 2011. Numerical simulation for the free surface flow around a complex ship hull form at different Froude numbers. *Alexandria Eng. J.*, 50: 229-235.
- Anonymous, 2017. User guide STAR-CCM. CD-adapco, Melville, New York, USA.
- Islam, H., M.M. Rahaman, H. Akimoto and M.R. Islam, 2017. Calm water resistance prediction of a container ship using Reynolds Averaged Navier-stokes based solver. *Procedia Eng.*, 194: 25-30.
- Olivieri, A., F. Pistani, A. Avanzini, F. Stern and R. Penna, 2001. Towing tank experiments of resistance, sinkage and trim, boundary layer, wake and free surface flow around a naval combatant INSEAN 2340 model. MSc Thesis, University of Iowa's College of Engineering, USA.
- Qiu, W., 2014. Report of the ocean engineering committee. Proceedings of the 27th International Conference on Towing Tank, September 4, 2014, ITTC, Copenhagen, Denmark, pp: 1-88.
- Querard, A., P. Temarel and S.R. Turnock, 2008. Influence of viscous effects on the hydrodynamics of ship-like sections undergoing symmetric and anti-symmetric motions, using RANS. Proceedings of the ASME 27th International Conference on Offshore Mechanics and Arctic Engineering, June 15-20, 2008, ASME, New York, USA., ISBN:978-0-7918-4822-7, pp: 683-692.
- Saha, G.K. and M.A. Miazee, 2017. Numerical and experimental study of resistance, sinkage and trim of a container ship. *Procedia Eng.*, 194: 67-73.
- Shia, A., M. Wu, B. Yang, X. Wang and Z. Wang, 2012. Resistance calculation and motions simulation for free surface ship based on CFD. *Procedia Eng.*, 31: 68-74.
- Wu, C., L. Yang, Z. Zhang, F. Zao and K. Yan, 2000. CFD simulation of Ship Model Free to Sinkage and Trim Advancing in Calm Water. In: Gothenburg 2000 Workshop On Numerical Ship Hydrodynamic, Larsson, L., F. Stern and B. Volker (Eds.). Chalmers University of Technology, Gothenburg, Sweden, pp: 435-440.